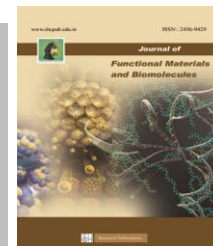




SACRED HEART RESEARCH PUBLICATIONS

# Journal of Functional Materials and Biomolecules

Journal homepage: [www.shcpub.edu.in](http://www.shcpub.edu.in)



ISSN: 2456-9429

## Investigation on the influence of reaction temperature on the optical properties of SnO<sub>2</sub> nanoparticles prepared by a simple hydrothermal route

A. Sabarinathan, M. Chinnathambi and R. Robert<sup>\*1</sup>

Received on 10 Dec 2018, Accepted on 31 Dec 2018

### Abstract

We report the influence of reaction temperature on the optical properties of Tin Oxide nanoparticles prepared using a simple hydrothermal method in aqueous medium. XRD results showed the formation of rutile tetragonal structure of the tin oxide nanoparticles with good crystallinity and the average crystallite size estimated from Scherrer formula varied between 28 to 33 nm for all the samples. The optical band gap of the SnO<sub>2</sub> nanoparticles prepared at 170, 180, 190 and 200°C is 3.85, 3.43, 3.21 and 3.02 eV respectively. The functional groups were identified by Fourier Transform Infra Red spectral analysis. The Transmission Electron Microscopy analysis has revealed that the prepared tin oxide nanoparticles are nearly spherical in shape with the actual particles size around 40 nm.

**Keywords:** Tin Oxide nanoparticles, hydrothermal method, Transmission Electron Microscopy.

### 1 Introduction

Nanomaterials have attracted great interest due to their intriguing properties, which are different from those of their corresponding bulk materials. In the past few years, tin oxide (SnO<sub>2</sub>) is an important n-type wide energy gap semiconductor (E<sub>g</sub> = 3.64 eV) which has a wide ranging applications such as in solid-state gas sensors for environmental monitoring [1-3], transparent conducting electrodes [4], rechargeable Li batteries [5], optical electronic devices [6], catalytic applications [7] and many more. To realize the aforesaid potential applications, very small particles of SnO<sub>2</sub> in the nanometric regime having large specific surface area is essential. Since the properties of nanoscale materials are strongly dependent on their size and shape, it is extremely desirable to be able to achieve size and morphology control during synthesis.

### 2 Experimental

#### 2.1. Material Synthesis

All chemicals were purchased from Merck and used as received without further purification and double distilled water was used throughout the synthesis process. Tin oxide nanoparticles were synthesized by simple

hydrothermal method, in which, 5.640g of SnCl<sub>2</sub>·2H<sub>2</sub>O and 5g of NaOH were dissolved separately in 25 ml double distilled water at room temperature with vigorous stirring for 15 minutes. When sodium hydroxide was added drop wise in the resultant solution, the milky white color of the solution has suddenly changed to light yellow and then into milky white as stirring continued. And as time progressed, the colour changed into light blue and finally the light blue color of the solution was changed to the deep blue due to the formation of tin oxide nano particles. Finally the solutions were kept in 150 ml teflon-lined stainless steel autoclave in different reaction temperatures (170, 180, 190 and 200 °C) for 24 hours and the precipitates were obtained. The resultant tin oxide precipitates were washed several times with ethanol and double distilled water. The precipitations were dried at 200°C for 3 hours using hot air oven.

### 3 Results and Discussion

#### 3.1. Powder XRD analysis

XRD is an instrumental technique that is used to identify the crystallite size of the materials. Structural analysis of the SnO<sub>2</sub> nano particles processed at different reaction temperature was carried out using Enraf Nonius CAD-F diffractometer with CuKα radiation source of wavelength (λ=1.54056 Å) and the diffraction patterns were recorded by varying diffraction angles in the range 10-80 degree. The crystallinity of the synthesised tin oxide powder is clearly manifested by the sharper diffraction peaks at their respective diffraction angles which can be readily indexed for its rutile tetragonal structure as given in fig.1. It can be seen that all the samples exhibit similar XRD profile, indicating the same crystal structure of SnO<sub>2</sub>. The obtained rutile phase is very much in agreement with the standard JCPDS data (JCPDS card no: 72-1012) [48]. The samples exhibited only the tetragonal rutile phase and the diffraction peaks around 2θ=18.3°, 29.82°, 33.26°, 37.12°, 47.78°, 50.72°, 57.4°, 62.5° and 69.89° are assigned to (001), (101), (110), (002), (200), (112), (211), (103) and (220) reflections. No diffraction peaks due to metallic Sn or other tin oxides are detected. Compared with those

\* Corresponding author e-mail: roberthosur@yahoo.co.in,  
Phone: +91 94439 82828

<sup>1</sup>Department of Physics, Government Arts College for Men, Krishnagiri, Tamil Nadu, India.

of the bulk counterpart, the peaks are relatively broadened, which further indicates that the prepared material has a very small crystallite size. The average crystallite size, estimated from XRD results using Scherrer formula is 28, 29, 30 and 33 nm with the increase of hydrothermal temperature. The variation of the grain size of SnO<sub>2</sub> nanoparticles with their corresponding reaction temperatures is depicted in fig.2.

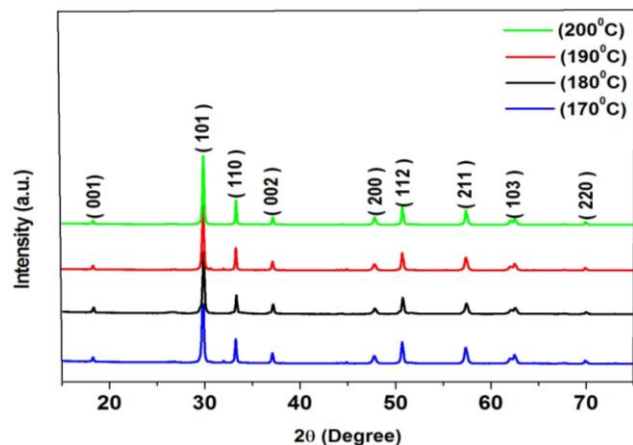


Fig.1. XRD patterns of SnO<sub>2</sub> nanoparticles prepared at different reaction temperatures

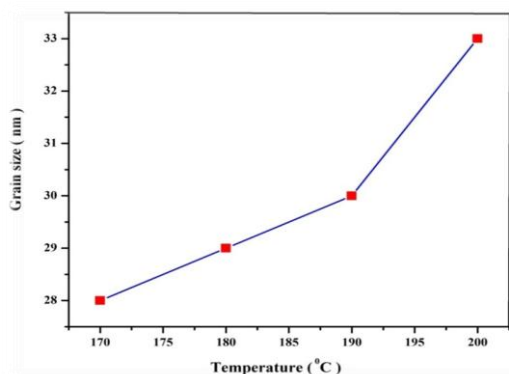


Fig 2. Dependence of mean grain size of SnO<sub>2</sub> for different reaction temperatures

### 3.2. UV-Vis absorption spectroscopy analysis

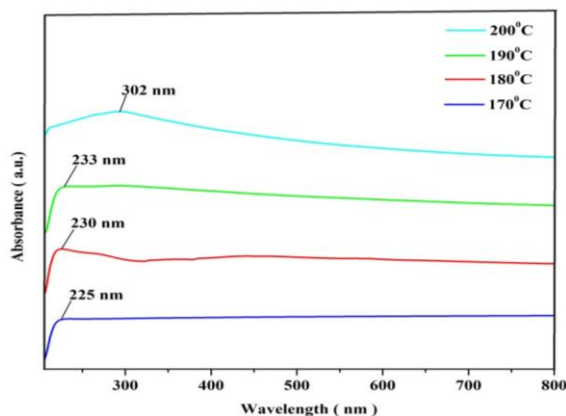


Fig.3. UV-Vis absorption spectrum of SnO<sub>2</sub> nanoparticles prepared at different reaction temperatures

The optical absorption spectra of SnO<sub>2</sub> nano particles prepared by hydrothermal route at different reaction

temperatures (170, 180, 190 and 200°C respectively) recorded using Lambda 35 UV-Vis spectrophotometer in the range 200–800 nm at ambient conditions are shown in fig.3. UV-visible spectroscopy is a method in which the outer electrons of atoms or molecules absorb radiant energy and undergo transitions to high energy levels. In this method, the spectrum obtained due to optical absorption can be analyzed to obtain the energy band gap of the semiconductor nanomaterials. In general, it was known that tin oxide nanoparticles have strong absorption peaks at about 200-400 nm. However, SnO<sub>2</sub> nano particles prepared by this method showed absorption peaks at 225, 230, 233 and 302 nm for the reaction temperatures 170, 180, 190 and 200°C respectively. These showed that a red shift occurred for the SnO<sub>2</sub> samples and it may be associated with the increase in particle size [49]. Considering the blue shift of the absorption positions from the bulk SnO<sub>2</sub>, the absorption onsets of the present samples can be assigned to the direct transition of electron in the SnO<sub>2</sub> nanocrystals. The optical band gap is calculated using Tauc plot with help of UV-Vis absorption spectrum. The band gap energy evaluated for the SnO<sub>2</sub> nanoparticles prepared at 170, 180, 190 and 200°C is 3.85, 3.43, 3.21 and 3.02eV respectively. This can be explained because the band gap of the semiconductors has been found to be particle size dependent. The band gap increases with decreasing particle size and the absorption edge is shifted to a higher energy (blue shift) with decreasing particle size.

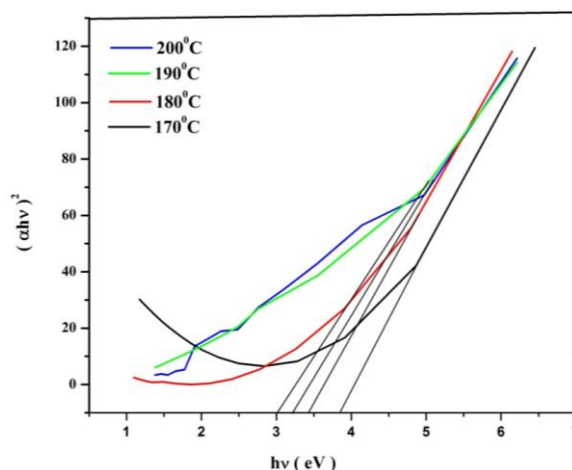


Fig. 4. Tauc plot for band gap energy in different reaction temperatures

The relation between  $\alpha$  and  $E_g$  for a direct transition is given by,

$$\alpha h\nu = A (h\nu - E_g)^n$$

where,  $\alpha$  is absorption co-efficient,  $h$  is Planck's constant,  $\gamma=c/\lambda$ , where,  $c$  is speed of light,  $\lambda$  is absorption wavelength,  $A$  is constant,  $E_g$  is band gap energy and  $n$  is equal to  $\frac{1}{2}$  for indirect transition semiconductor and 2 for direct transition semiconductors. From the above equation, we can see that  $(\alpha h\nu)^2$  has a linear relationship with  $h\nu$ . To calculate the band gap values of the prepared samples  $(\alpha h\nu)^2$  versus  $(h\nu)$  has been plotted and it is shown

respectively in the fig.4. The value of the band gap is determined by extrapolating the straight line portion of  $(\alpha h\nu)^2$  versus  $h\nu$  graph to the  $h\nu$  axis. The calculated band gap energies of the samples prepared at different reaction temperatures are 3.85, 3.42, 3.21 and 3.02eV respectively. The table showing the dependence of grain size on the band gap energy of the synthesized SnO<sub>2</sub> nano particles is given below.

Table 1 The dependence of grain size on the band gap energy of the SnO<sub>2</sub> nano particles

Reaction temperature (°C)	Absorption peak (nm)	Grain size (nm)	Band gap (eV)
170	225	28	3.83
180	230	29	3.43
190	233	30	3.21
200	302	33	3.02

### 3.3. FTIR analysis

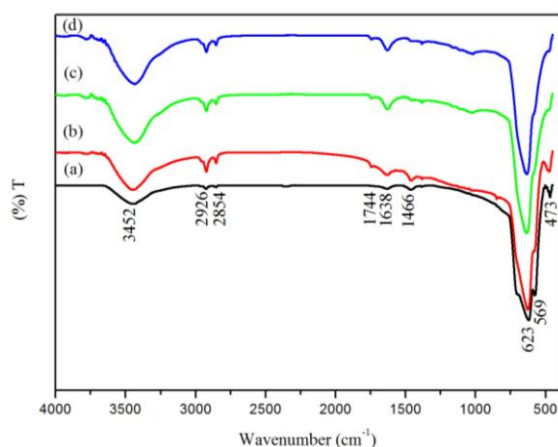


Fig.5. FTIR spectra of SnO<sub>2</sub> nanoparticles prepared at different reaction temperatures

FTIR spectrum of tin oxide samples prepared in different reaction temperatures (170, 180, 190 and 200 °C) are recorded in the range of 450-4000 cm<sup>-1</sup> at room temperature using Perkin Elmer Spectrum Two FTIR spectrophotometer and the recorded spectra are shown in the fig. 5. The absorption bands are observed at 473, 569, 623, 1466, 1638, 1744, 2854, 2926 and 3452 cm<sup>-1</sup>. The peak at 569 cm<sup>-1</sup> is related to Sn-OH vibration mode. A sharp absorption peak centered at 623 cm<sup>-1</sup> is assigned to O-Sn-O vibration mode indicating the transfer of the products to SnO<sub>2</sub> nanoparticles with good crystallization [50]. The peak at 1638 cm<sup>-1</sup> is assigned to the bending vibration of H-O-H bond from adsorbed water molecules [51]. The absorption band at 473 cm<sup>-1</sup> is attributed to stretching frequency in Sn-O [52]. The broad absorption peak at 3452 cm<sup>-1</sup> is due to O-H stretching vibration of surface hydroxyl group or absorbed water. The other various absorption bands are attributed to the O-H bond,

which come from the physical and chemical adsorbed water in the air [53].

### 3.4. TEM analysis

The Transmission Electron Microscopy (TEM) analysis was carried out to confirm the actual particles size and the morphology. Fig. 6 (a-d) shows the TEM images of the SnO<sub>2</sub> nanoparticles prepared in different reaction temperatures (170, 180, 190, and 200 °C respectively) using hydrothermal synthesis route. The particle size estimated by TEM micrographs is about 50 nm. It is likely that particles seen in the micrographs are composed of smaller particles as average crystallite size calculated by XRD was much smaller than deduced by TEM observations.

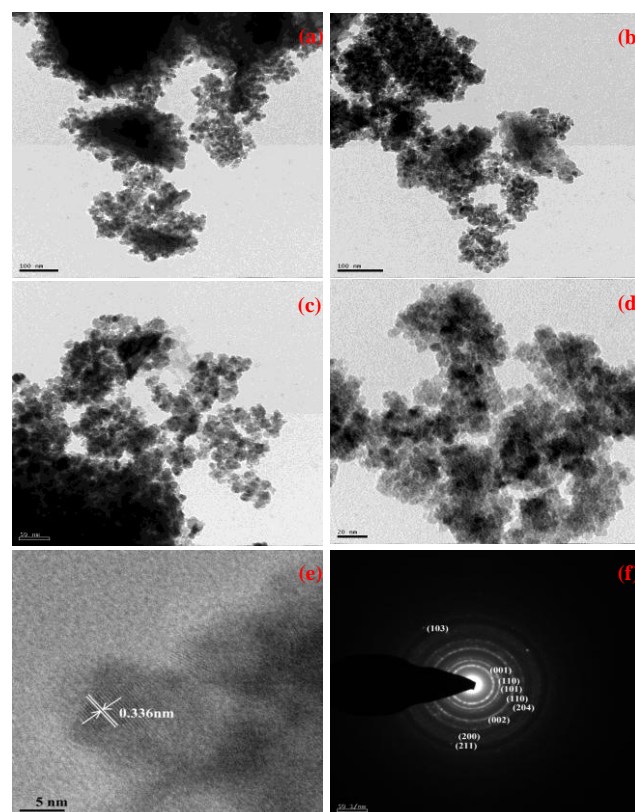


Fig.6. TEM micrographs of SnO<sub>2</sub> nano particles synthesized by reaction temperatures (a) 170°C (b) 180°C (c) 190°C (d) 200 °C (e) HRTEM and (f) SAED pattern

Fig. 5(f) represents the selected area electron diffraction (SAED) pattern taken from the SnO<sub>2</sub> nano particles for different reaction temperatures which can be indexed as a tetragonal rutile tin oxide in good agreement with the XRD results and it shows clear multiple diffraction rings patterns which suggest that the tin oxide nano particles are polycrystalline in nature. High-resolution Transmission electron microscopy (HRTEM) image obtained by deposition of a drop of the colloidal solution onto a carbon-covered copper grid gives further insight into the structural features of the prepared SnO<sub>2</sub> nano particles. From the HRTEM image of the sample (fig. 5(e)), one can observe clear lattice fringes with the interplanar spacing of approximately 0.336 nm,

corresponding to the (110) plane which was close to that of the tetragonal SnO<sub>2</sub> sample in agreement with the XRD data [54].

#### 4 Conclusions

The Tin oxide nanoparticles could be successfully synthesized by simple hydrothermal method. The nanostructured tin oxide nano powders were characterized by XRD, UV-Vis, FTIR and TEM analyses. XRD results showed good crystallinity of the samples and the rutile tetragonal structure of the tin oxide nanoparticles was confirmed. The average crystallite size, estimated from XRD results using Scherrer formula is around 28 to 33 nm for all the samples. The UV-Vis spectrum showed the absorption peaks at 225, 230, 233 and 302 nm and the optical band gap is calculated using Tauc plot with help of UV -Vis absorption spectrum. The band gap energy evaluated for the SnO<sub>2</sub> nanoparticles prepared at 170, 180, 190 and 200°C is 3.85, 3.43, 3.21 and 3.02eV respectively. The functional groups were estimated by FTIR analysis and the sharp absorption peak centered at 623 cm<sup>-1</sup> is assigned to O-Sn-O vibration mode indicating the transfer of the products to SnO<sub>2</sub> nanoparticles with good crystallization. The TEM analysis has revealed that the actual particles size is around 50 nm and the morphology of the prepared tin oxide nanoparticles is nearly spherical in shape.

#### References

- [1] Asim Umer, Shahid Naveed and Naveed Ramzan, "NANO: Brief Reports and Reviews", 7, 5, 123, (2012).
- [2] Li-Piin Sung, Stephanie Scierka, Mana Baghai-Anaraki, and Derek L. Ho, "Materials Research Society", Volume 740, 154 (2003).
- [3] Marcos Fernandez Garcia and Jose A. Rodriguez, "Brookhaven National Laboratory", Department of Chemistry, 79,479, (2007).
- [4] Hiromichi Hayashi and Yukiya Hakuta, "Materials", 3, 3794-3817, (2010)
- [5] Tsuyoshi Hamaguchi, Nobuaki Yabuki, Masayoshi Unoa, Shinsuke Yamanaka, Makoto Egashira, Yasuhiro Shimizu and Takeo Hyodo, "Sensors and Actuators B", 113, 852-856, (2006).
- [6] Li-Wei Chou, Yang-Yi Lin and Albert T.Wu., "Applied Surface Science" 277, 30-34, (2013).
- [7] H.N. Lim, R. Nurzulaikha, I. Harrison, S.S. Lim, W.T. Tan, M.C. Yeo, M.A. Yarmo and N.M. Huang, "Ceramics International" 38, 4209-4216, (2012).
- [8] Yu Lingmin, Fan Xinhui, Qi Lijun, Ma Lihe and Yan Wen, "Applied Surface Science" 257, 3140-3144, (2011).
- [9] Feng Gu, Shu Fen Wang, Meng Kai Lu, Yong Xin Qi, Guang Jun Zhou, Dong Xu and Duo Rong Yuan, "Inorganic Chemistry Communications" 6, 882-885, (2003).
- [10] Masoud Salavati-Niasari, Noshin Mir and Fatemeh Davar, "Inorganica Chimica Acta" 363, 1719-1726, (2010).
- [11] Fatemeh Davar, Masoud Salavati-Niasari and Zienab Fereshteh, "Journal of Alloys and Compounds", 496, 638-643, (2010).
- [12] A.R. Babar, S.S. Shinde, A.V. Moholkar and K.Y. Rajpure, "Journal of Alloys and Compounds", 505, 743-749, (2010).
- [13] P. Gateau, C. Petitjean, P.J. Panteix, C. Rapin and M. Vilasi, "Journal of Non-Crystalline Solids", 358, 1135-1140, (2012).
- [14] T.Krishnakumar, R.Jayaprakash, NicolaPinna, A.R.Phani, M.Passacantando and S.Santucci, "Journal of Physics and Chemistry of Solids", 70, 993-999, (2009).
- [15] Jingbo Mu, Bin Chen, Zengcai Guo, Mingyi Zhang, Zhenyi Zhang, Changlu Shao and Yichun Liu, "Journal of Colloid and Interface Science", 356, 706-712, (2011).
- [16] Jun Zhang, ShurongWang, YanWang, Mijuan Xu, Huijuan Xia, Shoumin Zhang,Weiping Huang, Xianzhi Guo and ShihuaWu, "Sensors and Actuators B", 139, 369-374, (2009).
- [17] Lexi Zhang and Yanyan Yin, "Sensors and Actuators B", 185, 594-601, (2013).
- [18] Jian-Ping Ge, Jin Wang, Hao-Xu Zhang, Xun Wang, Qing Peng and Ya-Dong Li, "Sensors and Actuators B", 113, 937-943, (2006).
- [19] Zhigang Wen, Feng Zheng, Hongchun Yu, Ziran Jiang and Kanglian Liu, "Materials Characterization", 76, 1-5, (2013).
- [20] Mingyu Wu,WenZeng and YanqiongLi, "Materials Letters",104, 34-36, (2013).
- [21] Liying Man, Jun Zhang, Jieqiang Wang, Hongyan Xu and Bingqiang CaO, "Particuology", 11, 242-248, (2013).
- [22] Nasrin Talebian and FarzanehJafarinezhad, "Ceramics International", (2013).
- [23] R. Rakesh Kumar, Mitesh Parmar, K. Narasimha Rao, K. Rajannaand and A.R. Phani, "Scripta Materialia", 68, 408-411, (2013)
- [24] H.N. Lim, R. Nurzulaikha , I. Harrison , S.S. Lim , W.T. Tan , M.C. Yeo, M.A. Yarmo and N.M. Huang, "Ceramics International", 38, 4209-4216, (2012).
- [25] Yanbao Zhao, Zhijun Zhang and Hongxin Dang, "Materials Science and Engineering", A359, 405-407, (2003).
- [26] Shudong Dai and Zhongliang Yao, "Applied Surface Science",258, 5703- 5706, (2012)
- [27] Zhigang Wen, Feng Zheng and Kanglian Liu, "Materials Letters", 68, 469-471, (2012)
- [28] Y.Q. Guoa, Y. Lia, R.Q. Tan and W.J. Song, "Materials Science and Engineering B", 171, 20-24, (2010).
- [29] C. Ararat Ibarguen, A. Mosquera, R. Parra, M.S. Castro and J.E. Rodriguez Paez, "Materials Chemistry and Physics", 101, 433-440, (2007).
- [30] Yue Li, Yanqun Guo, Ruiqin Tan, Ping Cui, Yong Li and Weijie Song, "Materials Letters", 63, 2085-2088, (2009).
- [31] Arham S.Ahmed, Ameer Azam, Muhamed Shafeeq.M, M.Chaman and S.Tabassum, "Journal of

- Physics and Chemistry of Solids”, 73, 943-947, (2012).
- [32] Xin Wang, Huiqing Fan and Pengrong Ren, “Colloids and Surfaces A: Physicochem. Eng. Aspects”, 402, 53- 59, (2012).
- [33] Kwang Min Lee, Doh Jae Lee and Hoon Ahn, “Materials Letters”, 58, 3122-3125, (2004).
- [34] Tao TAO, Qiyuan Chen, Hui ping Hu and Ying Chen, “Materials Chemistry and Physics”, 126, 128-132, (2011).
- [35] A.Gaber, A.Y.Abdel Latief, M.A.Abdel Rahim, Mahmoud and N.AbdelSalam, “Materials Science in Semiconductor Processing”, 16, 1784-1790, (2013).
- [36] Wen Zeng, Bin Miao, Qu Zhou and Liyang Lin, “Physica E”, 47, 116-121, (2013).
- [37] HuiChi Chiu and ChenSheng Yeh, “J. Phys. Chem C”, 111, 7256-7259, (2007).
- [38] Peng Sun, Yang Cao, Jun Liu, Yanfeng Sun, Jian Ma and Geyu Lu, “Sensors and Actuators B”, 156, 779-783, (2011).
- [39] Yue Li, Yanqun Guo, Ruiqin Tan, Ping Cui, Yong Li and Weijie Song, “Materials Letters”, 63, 2085-2088, (2009).
- [40] Yali Wang, Min Guo, Mei Zhang and Xidong Wang, “Scripta Materialia”, 61, 234-236, (2009).
- [41] Shudong Daia and Zhongliang Yao, “Applied Surface Science”, 258, 5703-5706, (2012)
- [42] G. Gaggiotti, A. Galdikas, S. KaEiulis, G. Mattogno and A. setlcus, “Sensors and Actuators B”, 24, 516-519, (1995)
- [43] Zheng Lou, Lili Wang, Rui Wang, Teng Fei and Tong Zhang, “Solid-State Electronics, 76, 91-94, (2012).
- [44] Yali Wang, Min Guo, Mei Zhang and Xidong Wang, “Thin Solid Films”, 518, 5098-5103, (2010).
- [45] Le Viet Thong, Le Thi Ngoc Loan and Nguyen Van Hieu, “Sensors and Actuators B”, 150, 112-119, (2010).
- [46] R.S.Khandpur, “Hand Book of analytical instrument”, 357, (2005).
- [47] Xiaoming Zhou, Wuyou Fu, Haibin Yang, Yunnan Mu, Jinwen Ma, Lecheng Tian, Bo Zhao and Minghui Li, “Materials Letters”, 93, 95-98, (2013).
- [48] R.Karslioglu, M.Uysal, and H.Akbulut, “J.Cryst.Growth”, 327, 22-26, (2011).
- [49] Y. Liu, F. Yang and X. Yang, “Colloids. Surf. A: Physicochem. Eng. Aspects”, 312, 219- 225, (2008).
- [50] S. Yang and L. Gao, J. “Am. Ceram. Soc”, 89, 1742-1744, (2006).
- [51] Korosi.L, Papp.S, Meynen.V, Cool.P, Vansant.E.F, Dekany.I, “Colloids Surf A”, 268, 147, (2005).
- [52] Jianrong Zhang and Lian Gao, “Inorganic Chemistry Commuications”, 7, 91-93, (20 04).
- [53] D.L. Chen and L. Gao, “J. Colloid Interface Sci.”, 278, 137, (2004).
- [54] Ning Du, Hui Zhang, Bindi Chen, Xiangyang Ma, Xiaohua Huang, Jiangping Tu, and Deren Yang, “Materials Research Bulletin 44, 211-215, (2009).